*Progress In Electromagnetics Research, PIER 49, 161–188, 2004*

# DEVELOPMENT OF A THREE BAND RADAR SYSTEM FOR DETECTING TRAPPED ALIVE HUMANS UNDER BUILDING RUINS

**M. Bimpas, N. Paraskevopoulos, K. Nikellis, D. Economou and N. Uzunoglu**

National Technical University of Athens
Department of Electrical and Computer Engineers
9 Iroon Polytechneiou Str, 15773, Zografou, Athens, Greece

**Abstract**—This paper shows the ability to use a continuous wave (CW) radar as an instrument to search for trapped alive persons in demolished buildings and ruins. The utilized operation principle is the detection of the Doppler frequency shift of the E/M wave when it is reflected by a slightly moving part of a living human body. The presented system has gone through several prototype development phases. Many parameters and alternative implementations have been tested in both real and simulated sites. A system analysis is carried out and presented followed by a presentation of the signal processing techniques. The inherent difficulties for the realization and practical exploitation of such a system are discussed. Results from tests of the system are also presented.

## 1. INTRODUCTION

It is very important to maximize the chances of detecting trapped persons in collapsed buildings, in a short time following a disastrous earthquake. Disaster situations also demands that the location of the trapped person be determined as precisely as possible, to assist rescue teams.

In past years, several researchers have suggested the use of CW Doppler radar to detect trapped living persons within collapsed buildings [1, 2]. However real world experience with such radars is rather limited. An early prototype version of the system presented in this article was used to assist rescue teams in the 7th September 1999 earthquake in Athens. The experience gathered in tests showed that both the enhancement of the penetration depth and the improvement in spatial resolution are required to increase the performance of life detector systems. Additionally it was made clear that the performance of the system would greatly benefit from the utilization of any advanced signal processing and visualization techniques.

A prototype Life Detector radar has been developed [3], in the Microwave and Fiber Optics Laboratory of the National Technical University of Athens, Greece (MFOL/NTUA). The result is a functional system named SOZON (meaning "saver" in Greek). Since 2001 experiments have been conducted with a triple frequency radar named SOZON II (P, S and X bands). Actually this new system consists of three similar RF transceivers, each one operated in a different frequency band. All share a common user interface. The various wavelengths offer different characteristics regarding penetration depth and sensitivity to slight motions.

As a result of the experience gathered from the test measurements carried out the last two years, the latest version of this radar system has been designed and reconstructed, using only a single frequency of 2.45 GHz, which was considered to be the most appropriate for such an application.

The operation principle of the radar system and some fundamental on Electromagnetic and Radar theory, parallel to some experimental measurements, are presented in Sections 2 and 3 respectively. The Signal Processing procedures used to detect trapped humans is presented in Section 4. In Section 5 a system description of the three-band detector is given, followed by experimental results in Section 6. The system description of the latest prototype, SOZON III, is presented in Section 7 and experimental results from this new system in Section 8. Sections 9 and 10 discuss the overall performance of the system and derive conclusions for the efficiency of the present system, and possible future improvements.

## 2. OPERATION PRINCIPLE

Even when a human person is unconscious, the interior organs of his/her body are in constant oscillatory motion. When a Continuous Wave (CW) electromagnetic signal of frequency $f_0$ hits a moving object (in present case the heart or the moving chest of the trapped person) the frequency of the scattered signal undergoes a Doppler frequency shift $f_d$, which is proportional to the relative radial velocity, $v_r$, of the object with respect to the transmitter following the law, and is computed by using the following relation:

$$f_d = 2\frac{v_r}{c} f_0 \tag{1}$$

where $c$ denotes the speed of light in the propagation medium.

In order to simplify the analysis the targeted human body is assumed to execute a sinusoidal oscillation having cyclic frequency $\Omega$.

Thus, the radial velocity can be described as:

$$v_r = v_{r0} \cdot \cos(\Omega \cdot t) \tag{2}$$

Consequently, the Doppler frequency shift is:

$$f_d = 2 \cdot \frac{v_{r0}}{c} \cdot f_0 \cdot \cos(\Omega \cdot t) \tag{3}$$

This indicates that $f_d$ shows a fluctuating behavior but with a constant period. Thus, the returned signal at the receiver has frequency $f_0 + f_d$, and the down converted signal at the baseband part of the receiver has the form:

$$s(t) = \alpha \cdot \cos(2\pi f_d \cdot t) \tag{4}$$

or equally:

$$s(t) = \alpha \cdot \cos\left(2\pi \cdot \frac{2v_{r0}}{c} f_0 \cdot \cos(\Omega t) \cdot t\right) \tag{5}$$

Experiments have shown that the spectrum of this waveform has a fundamental component between 0.5 and 5 Hz in case of humans. This fact is exploited as detection criterion.

## 3. PENETRATION DEPTH OF E/M WAVES IN MATERIAL MEDIA

In operating the three-band Life Detector Radar, the most critical parameter is the signal penetration depth. A review study of the electromagnetic theory was carried out [4], parallel to the experimental results obtained in test measurements [5]. The most difficult material of buildings for an electromagnetic wave to penetrate is iron loaded concrete. The case of metallic structures is not considered since penetration of electromagnetic waves is impossible. This result was derived from the experience of the initial use of the system.

It is well known that the penetration depth in a lossy half space can be computed by using Equation (6) [4]:

$$\delta = \frac{1}{\alpha} = \frac{1}{\omega\sqrt{\mu\varepsilon}\left\{\frac{1}{2}\left[\sqrt{1+\left(\frac{\sigma}{\omega\varepsilon}\right)^2}-1\right]\right\}^{1/2}} \tag{6}$$

where $\sigma$ denotes the conductivity of the media (in our case mainly concrete), $\mu$ is the magnetic permeability and $\varepsilon$ the dielectric permittivity of the material. It should be emphasized that (6) indicates the $1/\omega$ dependence of penetration depth to frequency.

Typical values of conductivity and relative permittivity for concrete are $\sigma = 10^{-3} - 10^{-1}$ S/m and $\varepsilon_r = 6 - 12$ respectively, mainly depending on the percentage of concrete humidity and the depth below surface [6, 7]. Moreover, several measurements concerning the measurement of attenuation (dB/cm) of E/M waves, considering concrete as the propagating media were conducted [5]. Indicative results for 10 GHz and 2.45 GHz frequencies are shown in Table 1.

**Table 1.** Attenuation of waves in concrete (X/S band) based on experimental results.

| | | |
|---|---|---|
| Humidity 4% | F=10 GHz → L=2.435dB/cm | F=2,45GHz → L=0.6dB/cm |
| Humidity 8% | F=10 GHz → L=3.935dB/cm | F=2,45GHz → L=0.98dB/cm |

## 4. SIGNAL PROCESSING

### 4.1. General

The Life Detector System ends with a signal-processing unit and the user interface. The user interface is a Windows software application that displays the signal, the Fourier transform, and an indication of the received signal amplitude, as shown in Fig. 1. The left graph is the time-domain signal, displaying time (in seconds) on the horizontal axis and voltage on the vertical. The right is the FFT, displaying frequency on the horizontal axis (in Hz) and squared magnitude on the vertical. Both graphs are scaled to the maximum value of the displayed function. There is also a display of detection criterion as defined in Section 4.3 at the right side of the FFT graph. Finally, a "history file" at the bottom side of the graphs for keeping the previous measurements is displayed. The interface allows the user to set the properties of the A/D converter, store and load a set of measurements and change several display attributes. Signal processing is embedded in this application and will be explained in detail in a later section.

Experimental observations show that the detected signals under real conditions are highly stochastic. It should be noted that the model of the radial velocity, as expressed in Eq. (2), is an oversimplified assumption. Neither the movement of the chest due to the body respiration process nor the heartbeat is sinusoid. Even for the sinusoid approximation though, parameters vary from person to

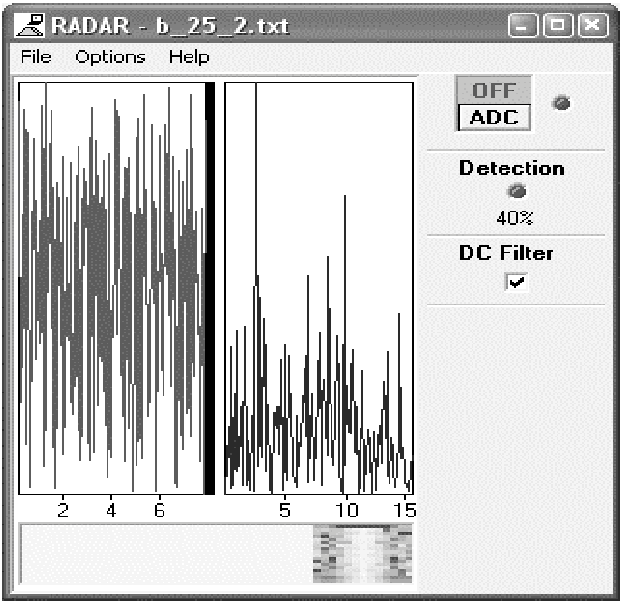


**Figure 1.** Screenshot of the user interface. Apart from the time domain signal and the FFT, there is also a display of the detection probability, as well as a "history file" at the bottom side of the graphs for keeping the previous measurements.

person. Additionally, they might change for a single person in different time instants. For example a frightened person might breathe faster, thus resulting in a greater frequency $\Omega$. If the same person calms after a while, the value of $\Omega$ drops. Additionally the position of the body with respect to the incident wave plays an important role in the amplitude of the signal. If the movement that should be observed is perpendicular to the wave propagation vector, then the radial velocity vanishes.

Another factor that can greatly deteriorate the performance of the system is the propagation loss. The majority of the materials used in buildings are lossy materials that attenuate signals so much that it might be rendered indistinguishable from noise. Media made of bricks and wood are easy to penetrate by electromagnetic waves, in contrast to concrete which is much harder, as displayed in Section 3.

Yet, a site examination of demolished buildings indicates that it consists of alternating layers of concrete and other types of rubble (bricks and furniture). Trapped people may be located under several layers of concrete, making it difficult for the electromagnetic wave to reach them and then return back to the antenna. On the other hand, cracks on the concrete slabs or any sort of poor building structures might help the wave propagation through it.

Other factors also affect system operation: Even minor movements of the antenna can produce such a strong signal that renders all useful signals indistinguishable from artifacts. Radiation leakage due to antenna sidelobes or random reflections may produce false alarms.

This stochastic nature of the signals results in difficulty to derive an automatic detection criterion. It follows that the experience of the operator of the system plays a significant role in the decision for the existence of target. Therefore the user interface is critical.

### 4.2. Fourier Transform Signal Processing

Tests of the early prototype of the system utilized an oscilloscope to display the output waveform. The limitations and inconveniences of this device made clear the necessity for a more advanced display and signal-processing algorithm.

The radar presented in this article uses a portable computer showing, not only the time domain signal, but also the Fourier transform. This addressed some of the problems of the oscilloscope. Additionally the process for calculating the Fourier transform of the sampled data involves integration. This enhances the signal to noise ratio.

### 4.3. Experimental Detection Criterion

Fast Fourier Transform (FFT) [8] approach is used to estimate the spectral density of the signal. Decision about the existence of trapped humans is taken by a subroutine which calculates and displays the portion of the energy of the signal that lies between 0.5 and 5 Hz. Experience in field tests showed that observations of a constant frequency component in this frequency range is a strong indication for the existence of a living person under the ruins. The term "detection criterion value" in the results sections refers to the ratio of the baseband signal energy included in the bandwidth between 0.5 Hz and 5 Hz to the total signal energy, always measured in the same integration time. The term "detection probability" is also mentioned in the results. It provides the probability of correct decision about the existence or non-existence of human, proportional to the total number of tests.

Later versions of the interface program include a graphical history of the Fourier transforms. This helps the operator to identify situations where a constant component at lower frequencies is present.

## 5. DESCRIPTION OF THE X-BAND (SOZON I) AND THE THREE-FREQUENCY RADAR SYSTEM (SOZON II)

The CW-Doppler radar is based on the principle of illuminating the moving body of the trapped person with a continuous wave signal and utilizing the frequency shift of the back-scattered signal [9]. The microwave, continuous wave CW signal, is generated by a Phase Locked Loop (PLL), filtered, amplified and finally transmitted by an antenna. The same PLL is also used as local oscillator in the receiver. A highly directive horn antenna of 26 dBi gain is employed in the higher frequency system (10.25 GHz) [10]. For the lower frequencies (2.45 GHz and 433 MHz) of the radar system, independent transmit/receive corner reflector antenna approach is employed to achieve the necessary isolation (higher than −50 dB) between transmitter and receiver for the P and S bands. For the higher frequency of 10.25 GHz the same horn antenna was considered efficient enough to be used.

The use of independent receive/transmit antennae with high isolation solved receiver saturation problems, due to reflection from the ground surface existing in the near-field of the antenna. In designing the 433 MHz and 2.45 GHz antennae, the HFSS-Agilent software package was used. In designing the 433 MHz and 2.45 GHz antennae, the HFSS-Agilent software package was used.

The block diagram of the radar systems operated at the lower frequencies is given in Fig. 2. The difference from the 10.25 GHz system is that the latter uses a single antenna configuration with a microwave circulator.

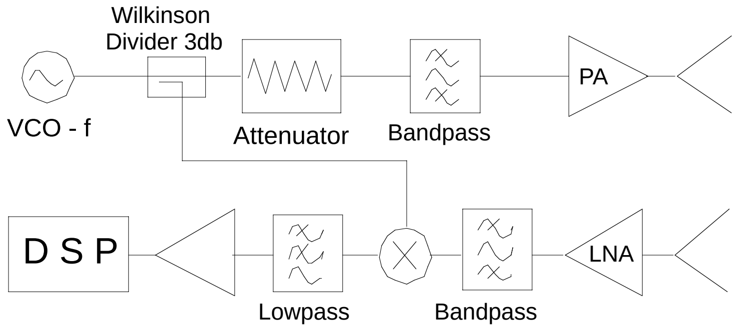


**Figure 2.** System block diagram of life detector for the lower frequencies of 433 MHz and 2.45 GHz consisting of three parts: antenna part, microwave circuit part and low frequency part.

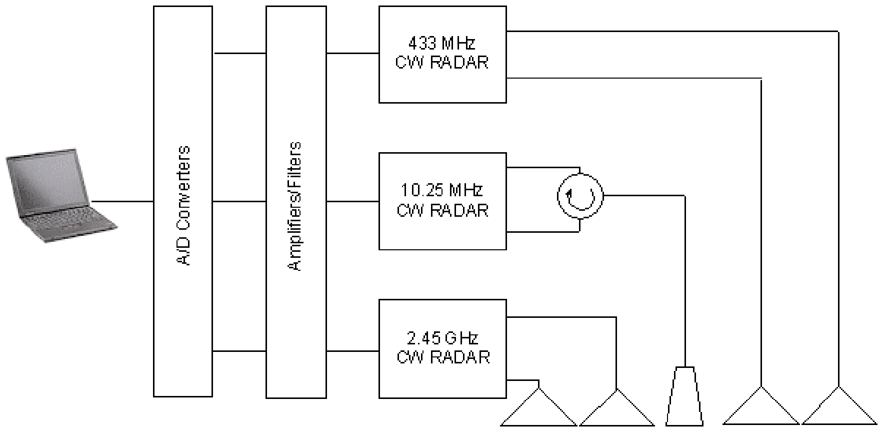


**Figure 3.** Schematic diagram of the three-band frequency CW-Doppler radar (the complete system SOZON II).

On the receiver side, a Low Noise Amplifier (LNA) following a microwave bandpass filter brings the signal to a power level that can be processed by the mixer. Since homodyne topology is employed, the mixers used are bipolar technology with low flicker noise, for better sensitivity. Due to the narrowband nature of the signal, the filters used in the baseband unit are implemented accordingly [9]. Digital processing is used to improve the signals.

The mixer output drives the baseband unit. The latter consists of an active, 4-pole, anti-aliasing lowpass filter with a cutoff frequency of 30 Hz, amplifiers and the A/D converter.

ADS and Momentum software packages from Agilent were used for designing the microwave circuits [12, 13], while Protel was used for the design of the low frequency components. Surface Mounting elements technology is utilized.

The block diagram of the three-frequency radar is presented in Fig. 3. The detected signals are amplified at each receiving channel after the down conversion. Then they are filtered and fed into a bank of A/D Converters, installed on the portable computer. This is operated as a signal processing and interface unit.

ADC42 of Pico Logic was used as A/D converter for our application, with the following characteristics given in Table 2.

In Fig. 4 a photograph of the X-band radar system (Sozon I) is presented. From right to the left the main part of the receiver and the transmitter plugged on the upper part of the antenna, the PC with the A/D converter and the baseband unit of the radar can be seen.

**Table 2.** Characteristics of the A/D converter ADC42 of Pico Logic.

| | |
|---|---|
| Resolution | 12 bits |
| Number of input channels | 1 |
| Input voltage range | –5 up to +5 Volt |
| Maximum sampling rate | 15 KSamples/sec |
| Typical error | ±1% at 25… C |
| Input resistance | 1 MΩ |

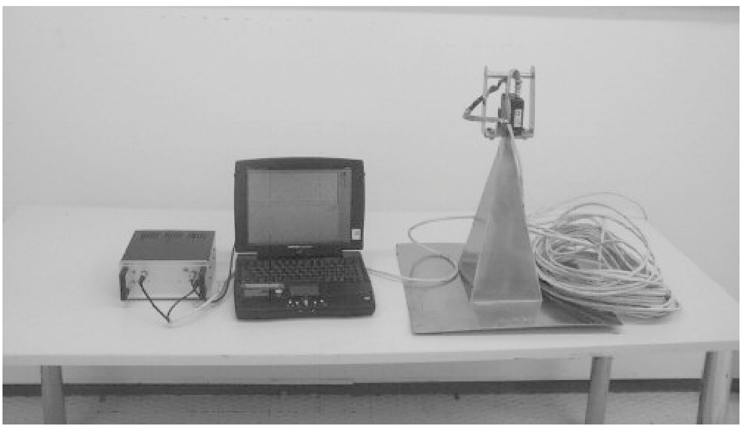

**Figure 4.** Photograph of the X-band radar system.

In Fig. 5 a picture of the three-frequency system (SOZON II) is presented. The inner view of this detector can be seen at the upper-right and lower-left corners. The portable PC and the antennas of this system can also be seen in this figure.

## 6. TEST RESULTS OF X-BAND (SOZON I) AND THREE-BAND (SOZON II) RADAR SYSTEM

### 6.1. Introduction

In order to assess the performance of the Life Detector System extensive tests were carried out at sites with characteristics as close as possible to those of collapsed buildings. The procedure used was

**Figure 5.** Photograph of the triple-frequency radar system.

placing the antennae of the system on the surface of an iron-loaded concrete slab (found either in building sites or in test sites) and the laptop approximately 10 meters away, to avoid detecting the operators of the system. Then measurements were taken, first without anyone under the concrete slab and then with a person lying under the slab. The sampling settings were 128 samples in 3 seconds (sampling frequency 42.67 sps). In cases where a more detailed waveform had to be acquired, 256 samples were taken in a period of 5 or 10 seconds. Setting the total sampling time to a high value allowed a better view of the lower frequencies, which are the most interesting for this system. The measurements were compared on site but also saved for further investigation.

## 6.2. Measurements Using the Initial Radar SOZON I

The most distinguishing feature of detecting living human presence is the prevailing low frequency components in the range of 0.5 to 5 Hz, persisting across measurements, as shown in Fig. 6. In addition to the time dependence of the detected signals, the FFT dependence to the Doppler shift frequencies is shown in Fig. 6. On the other hand, an

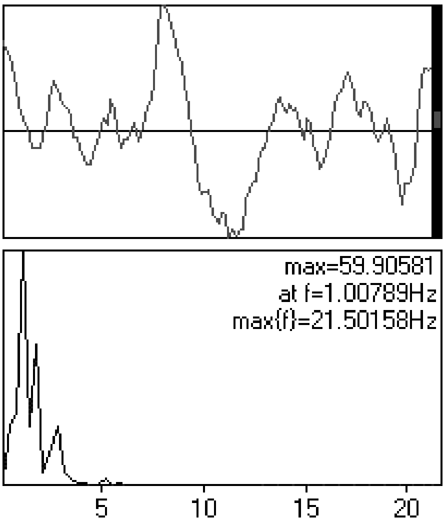


**Figure 6.** Screenshot from the interface of the system showing a case of an actual measurement with a living person under a thin concrete slab (left). On the right there is another case of an actual measurement with a living person. Time domain is on top, and frequency domain at the bottom.

irregular spectrum covering the entire bandwidth is observed in the absence of the human target as displayed in Fig. 7.

The maximum value of the magnitude, the frequency at which the maximum amplitude is observed, and the maximum frequency according to the sampling settings and the Nyquist theorem are extra data displayed, as shown in Figs. 6 and 7.

When the person is moving under the rubble, both the signal and the spectrum become irregular. In such cases a signal amplitude indicator is included in the interface, making it much easier for the user to judge whether the received signal is noise or a result of some movement.

Results from measurements are shown in Figures 6 and 7. They apply to the first version of the radar, that utilized only the 10.25 GHz frequency. Apparently this one gives excellent accuracy, being able to detect even a totally still person from the beat of the heart alone. However, it has the major drawback of low penetration depth, since the shorter wavelength can only penetrate a thin concrete slab. This was the main reason to develop another enhanced version of the radar system that utilizes additional lower frequencies.

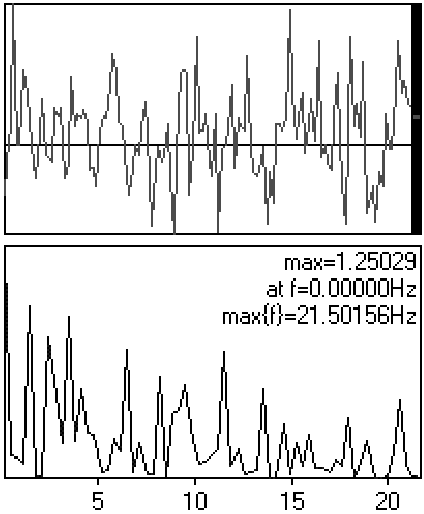


**Figure 7.** A measurement with no human.

### 6.3. Measurements Using the Improved SOZON II

In order to overcome the problem of the low penetration depth observed at the 10.25 GHz, the three-frequency radar was developed and a range of measurements was carried out with it. The lower frequency of 433 MHz showed a significant increase in penetration depth, as expected. However it could only detect large-scale movements of the body, such as an intensive movement of a hand. Some very characteristic recordings of such measurements are presented in Figures 8 and 9.

At the first row of the screenshots, the results coming from the X-band radar are presented, at the second row the results from the P-band, and finally at the third row the signal of 433 MHz. In any case there is the returned signal in time domain (on the left side), and also in frequency domain (on the right side). An indication of the strength of the received signal is also available to the radar operators from the indicator on the right edge of the time domain signal.

The screenshot of Fig. 8 depicts a case of a human lying under a slab of concrete of 30 cm thickness. All detection criteria are fulfilled, that is to say a sinusoidal signal waveform in time domain and frequency spectrum steadily concentrated below 5 Hz in the frequency domain. Moreover it is also worthy of remark that the amplitude indicator in all frequencies clearly indicated the increase of the amplitude of the signal in the presence of human. These visual

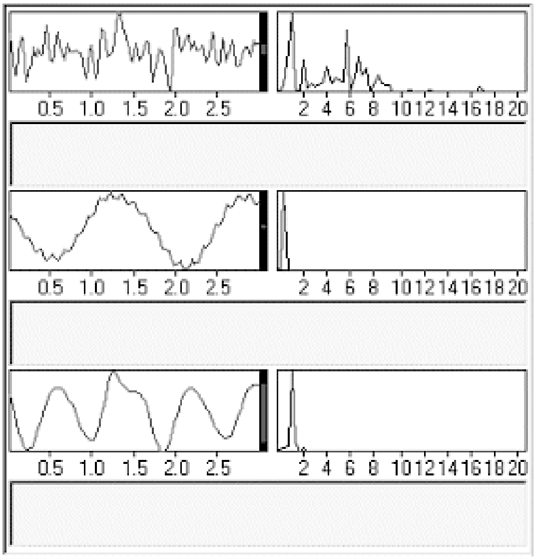


**Figure 8.** Three-band, person lying under a 30 cm concrete slab.

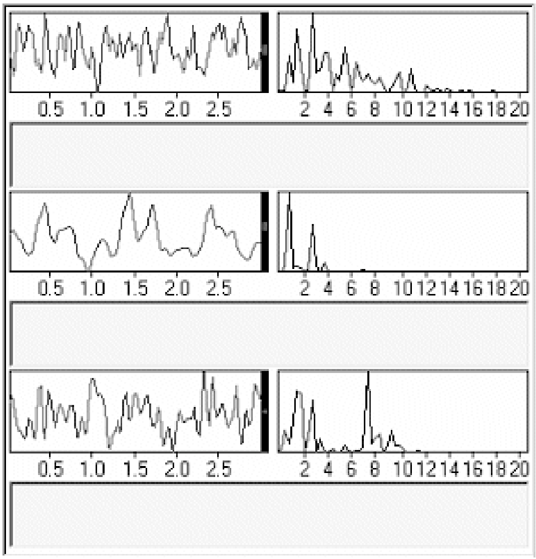


**Figure 9.** Screenshot of the triple frequency interface, in a case of a man lying under a 30 cm concrete slab. Some factor deteriorates the performance.

aids allow the radar operators to draw the conclusion that there is a human breathing under the rubble.

In Fig. 9, a case of uncertainty is depicted. This might be caused in case that either the trapped human does not lie exactly under the antennae of the radar system, or the man is totally unconscious resulting to a very slight chest movement, or even due to an external factor causing interference to our receiver. The results coming from the 2.45 GHz part though might lead to the conclusion of human existence. In such a case (which is the most usual case), the operators should make some additional measurements around this area, in order to draw a more definite and clear conclusion.

In real environment tests, electromagnetic waves must penetrate a relatively large depth of concrete, and then the echo signals reach the receiver significantly attenuated. The effect of movements in the surrounding space, collected by the side-lobes of the antennae can cause false alarms. A movement, like the one emanating from a working machine, creates certain frequency coefficients that can be easily filtered out. Random movements (e.g., leaves of the trees) are more difficult, since they tend to create an image similar with the noise overlapping the image of an existing trapped person. In order to overcome this problem, extra care should be taken in the antenna design (to reduce the side lobes), as well as in signal filtering during the measurement process.

## 7. DESCRIPTION OF THE ENHANCED VERSION OF LIFE DETECTOR RADAR SYSTEM (SOZON III)

Based on the measurement results of SOZON I and II, a new enhanced system has been designed and constructed, in order not only to overcome most of the drawbacks of the previous systems, but also to obtain a more convenient and user-friendly form.

The results from the measurements, presented in Section 6, indicate:

- The X-band radar system has an excellent spatial accuracy of detecting very slight movements of captured persons, with limited penetration depth, especially concerning materials, such as concrete.
- The system operating at 433 MHz shows a much higher penetration depth, but it could only detect large-scale movements of human body, such as an intensive movement of a hand.

Based on these conclusions, the last version of the radar system, SOZON III, was chosen to operate at the carrier frequency of 2.45 GHz. The frequency 2.45 GHz combines a relatively good penetration depth with a satisfactory high spatial resolution. However, for experimental and researching reasons the prototype system was designed and constructed with a sufficient bandwidth around the frequency 2.45 GHz, so that the user of the system will be able to "scan" a range of frequencies and "choose" the best operational frequency. Furthermore, depending on the propagation medium, the transmitted power can be easily chosen by the user, by switching the variable attenuator. The transmitted power of SOZON III is approximately 2 Watts. The block diagram is given in Fig. 10.

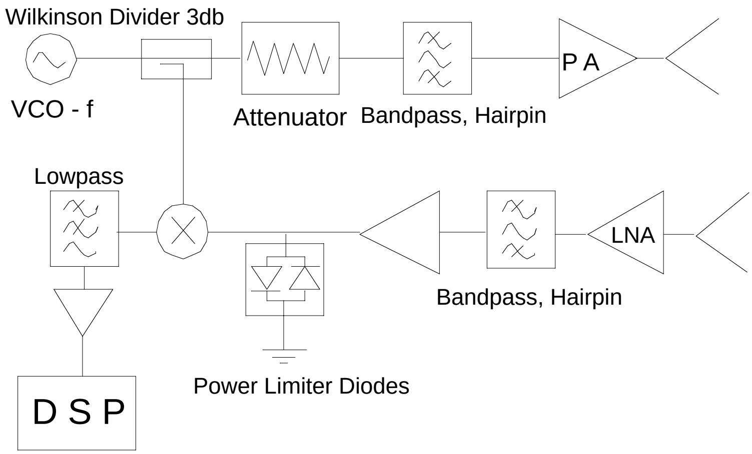


**Figure 10.** Block diagram of 2.45 GHz radar system (SOZON III).

The main differences of SOZON III compared to the previous generation systems, as far as the RF parts are concerned, are the following:

1. A prototype microstrip rectangular patch antenna was designed and developed (making use of additional parasitic patches and a slotted ground plane for enhanced gain, approximately 10 dB @ 2.5 GHz, as well as a dielectric cover for protection from ground surface roughness) for both receiver and transmitter, [14–16]. A more elaborative description of this antenna is going to be presented in a follow up paper.
2. It is important to emphasize on the optimized antenna's radiation pattern, in the great majority of the materials (concrete, brick walls, various types of soil), in which the E/M wave might be propagated in real conditions. A more elaborative description of this antenna will take place in a follow-up paper. In the antenna

design, simulations were carried out considering the existence of ground in the near-field of the antenna. Hence, the antenna performance was not drastically affected by the presence of the ground.

3. A low noise sensitive amplifier (LNA with $N_f = 2\,\text{dB}$ @ $2.5\,\text{GHz}$), followed by one more RF amplifier was used, in order to amplify very weak signals ($< -90\,\text{dBm}$). Due to the high gain of the LNA ($45\,\text{dB}$), the noise figure of the entire system is approximated by the noise figure of the LNA, according to Eq. (7) [17].

$$N_f = N_{f1} + \frac{N_{f2} - 1}{G_1} + \frac{N_{f3} - 1}{G_1 G_2} + \dots + \frac{N_{fm} - 1}{G_1 G_2 \dots G_{m-1}} \tag{7}$$

where $N_f$ is the noise figure of $N$ networks in cascade, and $N_{f1}$ and $G_1$ is the noise figure and available gain, respectively, of the first network (in our case Low Noise Amplifier), $N_{f2}$ and $G_2$ are the similar parameters for the second network (in our case Band Pass Hairpin Filter) and so on.

4. A pair of limiter diodes was used as a power limiter, to protect the microwave mixer of the receiver from high-power signals, which might intrude the receiver and subsequently cause damage to the system.

The most important characteristics of this radar are presented in the following table:

**Table 3.** Characteristics of the improved 2.45 GHz RADAR.

| | |
|---|---|
| Operation Principle | Continuous Wave@2,45GHz |
| Transmit power | 2 Watt |
| Minimum Power of the Received signal | –110 dBm |
| Receiver Noise Figure | 2 dB |
| Voltage Supply | +12 Volts |
| Power Consumptions | < 5 Watts |

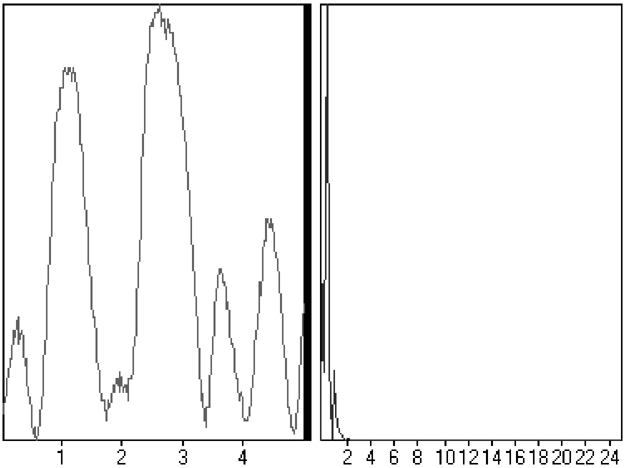


**Figure 11.** Measurement clearly indicating the existence of a human person.

## 8. TEST RESULTS OF THE ENHANCED VERSION OF SOZON III

### 8.1. Introduction

In order to assess the performance of the enhanced Life Detector System (SOZON III) extensive tests were carried out at sites with characteristics as close as possible to those of collapsed buildings. The procedure followed was the same as the previous described (in Section 6, Subsection 6).

### 8.2. Measurements Carried out Using SOZON III

In the following Figures 11, 12 and 13 some screenshots from measurements carried out using the latest version of the system are presented. Again the criterion is the sinusoid time-domain waveform and the prevailing low frequency components in the range of 0.5 to 1 Hz.

Figure 11 shows a case where the person behind the concrete slab (with thickness approximately 25 cm) is moving his entire body back and forth in the direction of the incident wave, thus resulting in maximum radial velocity. The frequency of this movement is higher than that of normal respiration, but the principle is the same.

This new system gave remarkable results in the case that no

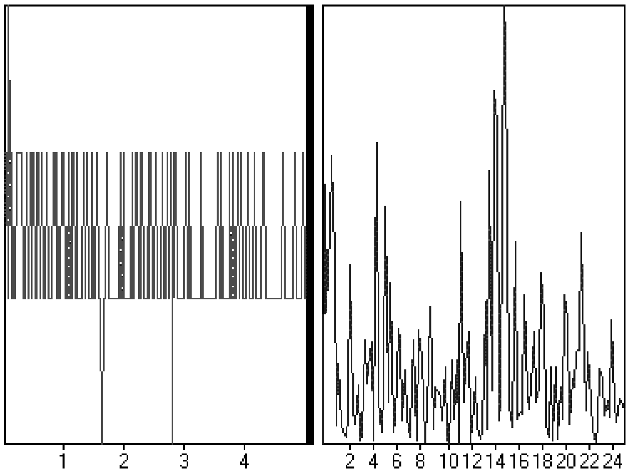


**Figure 12.** Measurement without a person.

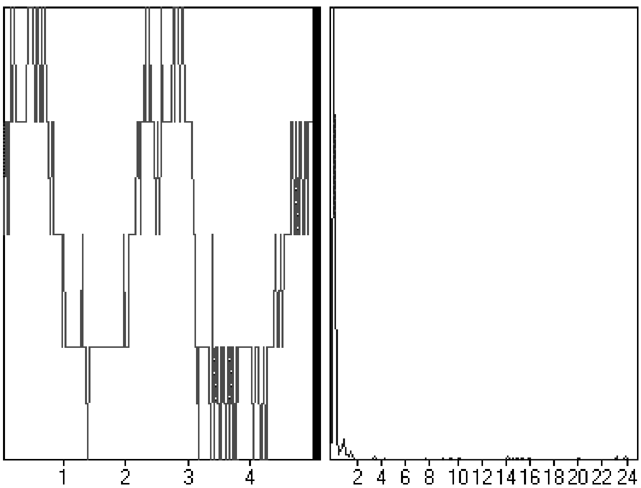


**Figure 13.** Person standing absolutely still.

human existed in the radar's field of view, as in Fig. 12. The time domain signal consists only of A/D converter noise. In the frequency domain, there is a totally irregular spectrum, which clearly indicates the absence of human under the concrete slab.

Equally remarkable is the case of a human standing perfectly still, as depicted in Fig. 13. In this case the person was even holding his breath. The strength of the signal is close to the resolution of the A/D converter, as indicated by the quantization of the voltage levels. However the sinusoid waveform, which is the main detection criterion, can be easily discerned, as shown in time domain graph of the screenshot in Fig. 11. The very low frequency component is emanated from the imperceptible movements of the human body, even when the person is perfectly still.

## 9. DISCUSSION ON THE TEST RESULTS

### 9.1. Introduction

In order to determine the extent of the system improvement in human detection under building ruins, it was considered essential to make some measurements using at the same time and under the same circumstances both the three-frequency and the 2.45 GHz Life Detector radar systems. Indeed, there was a comparison on the performance of the intermediate frequency of SOZON II and SOZON III.

After having tested the efficiency of the system, many measurements were carried out to assess the ability to detect trapped humans, in case that the antennae of the system were not located exactly directly above human target. Results are presented in the following.

Finally the effects of various building materials (e.g., bricks and concrete with different thicknesses) on the detection probability of the presented systems have been intensively investigated and presented in this section.

### 9.2. Effect of Antenna Location with Respect to the Trapped Person

In order for the system to be useful in real conditions, it is straightforward that the collapsed building surface has to be scanned effectively. This means that not only the trapped human beings must be detectable in a sufficient practical depth, but also that the total scan time must be kept as short as possible. The fundamental factor for determining the total scan time for an entire building is the distance by which the antennae can be moved to take the next measurement set. In case that this distance is too short, a lot of time will be needed to scan the entire building. In other words the whole system would be impractical for use.

Therefore it is evident that the antenna beams should be wide enough so that a larger area can be covered in one measurement. This minimizes the total time of measurements. This is a design tradeoff as a

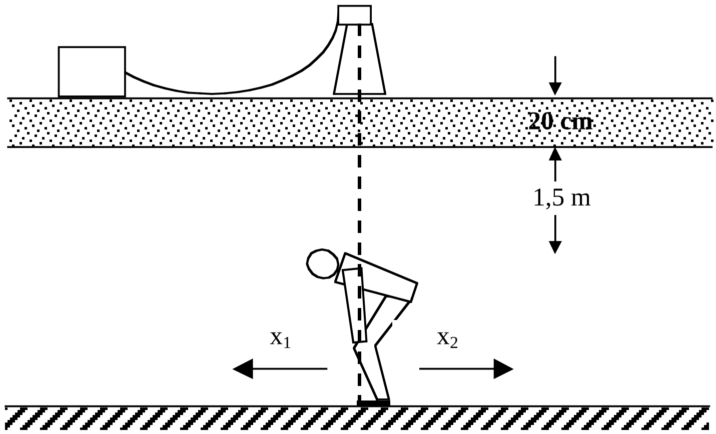


**Figure 14.** Schematic of the measurement procedure followed throughout the Life Detector Radar systems' testings.

wider beam also means lower antenna gain, resulting in less penetration depth.

In Fig. 14 the measurement procedure is presented. The antennae of the system were placed on the upper floor of a building, while the man was either standing bend or lying on the lower floor, so that the radar could detect his/her heart and chest movement. This methodology was preferred because it seems to have many similarities compared to real condition measurements, where trapped human beings lying under building ruins should be detected. The thickness of the existing concrete was 20 cm to 40 cm. The distance H between the lowest part of the ceiling and the persons back, fluctuated between practically 0 centimeter (corresponding to the case that person's back was adjacent to the ceiling) and a maximum of up to 1.5 meter.

Table 4 summarizes the detection criterion value versus antenna displacement from the center of the trapped human. The detection criterion is the one described in Section 4, Subsection 4.3. In the second and the third row of the Table 4 values of the detection criterion for SOZON II and SOZON III respectively are presented.

The first column, where displacement is 0, displays the average of the detection criterion value in case that the human is standing under a thin obstacle directly below the antenna. In every case, the value of the criterion deteriorates as the distance increases, regardless of the material media, the thickness of this material $D$ and the distance $H$.

For the results presented in Table 4, the concrete thickness $D$ of the ceiling used throughout the testing procedure was approximately

**Table 4.** Effect of antenna displacement on the detection criterion for SOZON II and SOZON III (concrete thickness $D = 25\,\text{cm}$, and distance $H = 5\,\text{cm}$).

| **Lateral Displacement x or x (m)** | 0 | 0.25 | 0.5 | 0.75 |
|---|---|---|---|---|
| **Detection Criterion for SOZON II** | 0.78 | 0.7 | 0.6 | 0.5 |
| **Detection Criterion for SOZON III** | 0.9 | 0.65 | 0.5 | 0.25 |

25 cm, while the value of $H$ was approximately 5 cm. The person who was standing under the concrete slab was totally still, in order to test the limits of both systems. If either the value of the concrete thickness $D$, or the value of the distance $H$ increased, the result was a respective decrease of the detection criterion for both systems.

As shown in Table 4, the detection criterion value for SOZON III is 0.9 (90%) whereas for SOZON II is 0.78 (78%), in the case that the antenna is directly above the person. On the other hand for displacements greater than 0 m, it is apparent that the detection criterion is better for SOZON II than for SOZON III. This is due to the differences in the characteristics of the antenna's radiation pattern between the two antennae used.

It is also remarkable that in the last case, which corresponds to the maximum displacement (approximately 0.75 m), none of the systems could provide a trustworthy decision for the existence of still persons. In case of SOZON III the same conclusion applies even for displacements higher than 0.4 m. This is because this value is only slightly above the observed value in the absence of a human. Therefore a decision about the presence of human is no more straightforward, as in the first case.

## 9.3. Detection Probability for Various Material Media

Finally it was considered essential to follow a similar procedure described in the previous subsection, for various types of materials existing between the antennae and the trapped person. Additionally the system was tested with different values of material thickness, aiming not only to confirm the theoretical and experimental results (presented in Section 3) but also to test the limits of the presented radar systems. The systems were tested making use of plastic furred wall, brick wall, insulated wall with double row of bricks, and of course concrete slabs with increasing thickness, as shown in Table 5.

**Table 5.** Average value of detection probability for various types of materials.

| Material | Detection Probability for SOZON II | Detection Probability for SOZON III |
|---|---|---|
| Furred wall | 0.98 | 0.99 |
| Brick wall | 0.95 | 0.98 |
| Brick wall (double) | 0.90 | 0.96 |
| Concrete slab 20cm | 0.82 | 0.92 |
| Concrete slab 25cm | 0.78 | 0.90 |
| Concrete slab 30cm | 0.72 | 0.85 |
| Concrete slab 35cm | 0.67 | 0.80 |
| Concrete slab 40cm | 0.61 | 0.75 |
| Concrete slab 50cm | 0.50 | 0.65 |
| Concrete slab 60cm | 0.35 | 0.55 |

The triple frequency radar system (SOZON II) gave satisfactory results in all the aforementioned cases including concrete slabs with thickness less than 30 cm. For higher values of concrete thickness a decrease in reliability, as well as a greater difficulty of drawing conclusions started to appear in both signal purity and the detection probability. Finally for values of concrete thickness greater than 40 cm it was impossible to detect the human motion. In the following Table 5 the average value of detection probability is presented for all the above cases. (in case of concrete slabs seven cases were discerned).

The enhanced radar system gave satisfactory results even in harder conditions, where the thickness of concrete slab exceeded 35 cm and the person who was standing under the slab remained perfectly still. This is due to the optimized redesign of 2.45 GHz radar system and especially the additional use of both the Low Noise Amplifier (LNA) and the RF amplifier, in the RF section of the receiver.

It is essential to mention again that the value of the detection criterion in case of a human absence was around 0.60 (lower values mean absence, higher mean presence). Thus, in all the cases that the detection criterion value is near 0.60 are cases of ambiguity.

Table 6 provides a summary of the typical values of the penetration depth for the various systems. Detection depth symbolizes not the penetration depth of the E/M waves, as defined in Eq. (6), but the width of concrete between the trapped person and the antenna of the system for which results are reliable.

**Table 6.** Typical values for the penetration depth for the various systems, referring to concrete.

| System | Sozon I | Sozon II | | | Sozon III |
|---|---|---|---|---|---|
| | 10.25 GHz | 433 MHz | 2.45 GHz | 10.25 GHz | 2.45 GHz |
| **Detection Depth (cm)** | 20 | 80 | 50 | 20 | 60 |

### 9.4. Effect of Environmental Factors on the Measurements

The final comparative measurements of the described systems concerned their effectiveness in detecting trapped human beings in noisy environments, and especially in case of moving persons close to the point of measurements. As it is mentioned in Section 6.3, the effect of human motions on the measurements of SOZON II was the main disadvantage of this system. In order to eliminate this drawback, the corner-reflector antennae of SOZON II were substituted with the prototype patch-antennae (described in Section 7) in the new enhanced radar system. This change played a catalytic role to system improvement since environmental motions around the point of measurements (e.g., human movements, or the motion of the tree branches, etc.) do not significantly affect the efficiency of SOZON III, compared to the previous system SOZON II.

## 10. CONCLUSIONS

The use of three independent radar sensors provides a significant improvement of detection probability and at the same time reduces the possibility of false alarm. This is due to the correlation of the output data carried out by the user. Additionally the three-band system allowed the evaluation of the suitability of the various bands for such an application. The most promising frequency proved to be 2.45 GHz, or even slightly lower than that, but well above the 433 MHz.

Thus, the latest version of the Life Detector Radar operating at 2.45 GHz was designed and constructed. The test results clearly indicated an improved system performance in detecting trapped human beings under building ruins. The effect of deteriorating environmental factors was eliminated since the new antenna design has very low leakage due to sidelobes. At the same time weaker signals could be detected and processed, due to the optimized design and construction of the electronic parts of the radar.

In order to achieve simplicity, portability and cost issues the new enhanced version of the Life Detector Radar System makes use of just one frequency 2.45 GHz. This frequency band is free for use by commercial applications, so we expect a minimum interference with other devices during our tests. More experiments are being conducted in the 1.8 GHz to 2.4 GHz range for designating the most suitable frequency, in order to further improve the performance of the system. After a thorough examination of the experimental results it is highly likely to change the operational frequency of the Life Detector system in the optimal range mentioned above.

It is essential to mention that all the systems developed make use of an homodyne topology, employed due to the requirements for low-cost application, as well as for simplicity and reliability reasons. However, heterodyne signal reception could also be utilized to improve the clutter rejection and achieve better sensitivity in a future enhanced version of the Life Detector System.

Another point worth of further research is the signal-processing algorithm. The detection criterion was derived purely from practical use, and would benefit greatly from a more thorough research.

## ACKNOWLEDGMENT

The authors wish to acknowledge the assistance and support of all those contributed to our effort to enhance and develop the described radar system, especially Dr. Yiorgo Stratako and the dipl. engineer Yiorgo Mitropoulo for their valuable help throughout the design, construction and testing of the RF parts of the radar.

## REFERENCES

1. Chen, K. M., D. Misra, H. Wang, H. L. Chueng, et al., "An X-band M/W life-detection system," *IEEE Trans. Biomedical Eng.*, Vol. BME-33, 697–701, July 1986.
2. Aggelopoulos, E. G., E. Karabetsos, Constantinou, and N. Uzunoglu, "Mobile microwave sensor for detection of trapped human beings," *Measurement: Journal of the International Measurement Confederation*, Vol. 18, No. 3, 177–183, July 1996.
3. Bimpas, M., K. Nikellis, N. Paraskevopoulos, D. Economou, and N. Uzunoglu, "Development and testing of a detector system for trapped humans in building ruins," *Proceeding of 33rd European Microwave Conference*, 999–1002, October 2003.

4. Balanis, C., *Advanced Engineering Electromagnetics*, John Wiley & Sons, Inc., 1989.
5. Measurement data provided by the Laboratory of Electronics, Antennas and Telecommunications, Ch. Pichot, University of Nice-Sophia Antipolis, France.
6. Davis, J., S. G. Millard, Y. Huang, and J. H. Bungey, "Determination of dielectric properties of insitu concrete at radar frequencies," *NDT-CE, 2003, International Conference*, Berlin, June 2003.
7. Soutsos, M. N., J. H. Bungey, S. G. Millard, M. R. Shaw, and A. Patterson, "Dielectric properties of concrete and their influence on radar testing," *NDT&E International*, Vol. 34, 419–425, 2001.
8. Press, W. H., S. A. Teukolsky, W. T. Vetterling, and B. P. Flannery, *Numerical Recipes in C*, 2nd edition, Cambridge University Press, 1992.
9. Skolnik, M. I., *Introduction to Radar Systems*, 2nd edition, McGraw Hill College Div, 1980.
10. Balanis, C. A., *Antenna Theory, Analysis and Design*, 2d edition, 682–695, 727–752, John Wiley & Sons, Inc., 1997.
11. Chalkias, C. and I. Papananos, *Design of Electronic Filters*, 1st edition, Symmetria Publishers, 1987.
12. Uzunoglu, N. K., *Introduction to Microwave Theory*, 2nd edition, Papasotiriou Publications, 1994.
13. Mongia, R., I. Bahl, and P. Bhartia, *RF and Microwave Coupled-Line Circuits*, Artech House Publishers, 1999.
14. Wong, K.-L., *Compact and Broadband Microstrip Antennas*, John Wiley & Sons, 2002.
15. Kumar, G. and K. C. Gupta, "Directly coupled multiple resonator wide-band microstrip antennas," *IEEE Trans. Antennas Propagat.*, Vol. 33, 588–593, June 1985.
16. Kumar, G. and K. C. Gupta, "Nonradiating edges and four edges gap-coupled multiple resonator broad-band microstrip antenna," *IEEE Trans. Antennas Propagat.*, Vol. 33, 173–178, Feb. 1985.
17. Kapsalis, C. and P. Kottis, *Antennas and Wireless Links*, Tziola Publications, 2003.

**Bimpas Matthaios** was born in Athens on January 2, 1978. He graduated from the Department of Electrical and Computer Engineering from the National Technical University of Athens in June 2000. Since February 2001, he is working towards a Ph.D. in Microwaves Laboratory of DECE/NTUA, on RF and antenna design and testing. His Ph.D. research focuses on system design, as well as RF modules and antenna design and measurements for radar applications, and mainly ground penetrating radar (GPR) applications. His research interests include EMI/EMC issues, H/W and S/W engineering for sensors, mobile communications and telematic applications. He has worked in several European and national projects. He has published 6 papers in Conference proceedings and attended 3 seminars on antenna design and EDA tools and 3 international conferences.

**Nikolaos Paraskevopoulos** was born in Athens in 1977. He graduated from the National Technical University of Athens, department of Electronics and Computer Engineering, in 2000. His studies mainly focused on computer systems architecture and communication systems. Currently he is working towards his Ph.D. in RADAR signal processing in the Microwave and Fiber Optics Laboratory of the National Technical University of Athens. His interests range from digital signal processing and embedded systems applications to high level software engineering.

**Konstantinos Nikellis** was born in Mytilini, Greece, in 1977. He received his diploma in electrical engineering from the National Technical University of Athens (NTUA) in 2000, and he is currently working towards his Ph.D. degree in electrical engineering at the NTUA. His main interests are RF IC design of silicon RF ICs and the development of novel modeling methods for on-chip and in-package RF structures. Currently his main areas of research are microwave & RF circuit design and numerical E/M simulation of microwave structures.

**Dimitris P. Economou** was born in Athens, Greece in 1972. He received Dipl.Elec.Eng. in 1995 and the Ph.D. degree in Applied Electromagnetics in 2001 from the Electrical Engineering Department, National Technical University of Athens. He was the head of RF group in the Institute of Accelerating Systems and Applications, Athens, Greece from 1997 to 2002. He is currently co-founder and technical director of EPOS SA, Athens, Greece.

**Nikolaos K. Uzunoglu** is Professor of the School of Electrical and Computer Engineering (SECE) at National Technical University of Athens (NTUA) from 1987. He holds a Degree in Electrical and Computer Engineering from Polytechnic University of Instanbul (1973), a M.Sc. in Quantum Electronics (1974) and a Ph.D. in Microwaves ("Theoretical Calculations of Scattering of Electromagnetic Waves from Precipitation Particles") (1976) from University of Essex and a postdoc at NTUA (1982). He has served as President of SECE for 6 years (1986–1992) and as Director of the Institute of Communications and Computer Systems/NTUA from 1992–1999. He is Head and Technical Manager of Microwave and Fiber Optics Lab while he has been Scientific Co-ordinator in more than 100 national and European programs. His research interests are in the field of Microwave and Fiber Optics Telecommunications, wireless Telecommunications, Radar Systems and Remote Sensing, applications of Electromagnetic Theory and Biomedical Engineering, Microwave and Field Measurements. He has published over 200 papers and articles in Conference Proceedings with evaluation process and International Journals, 3 scientific books and more than 200 technical reports. He was given the International G. Markoni award in 1981 and he is a Member of IEEE, of the Technical Chamber of Greece and National Representative for the European Union Cost Telecommunications programs.